Angiogenesis **6**: 55–64, 2003.

Caldesmon-dependent switching between capillary endothelial cell growth and apoptosis through modulation of cell shape and contractility

Yasushi Numaguchi[1], Sui Huang[1], Thomas R. Polte[1], Gabriel S. Eichler[1], Ning Wang[2] & Donald E. Ingber[1]

[1]*Vascular Biology Program, Departments of Pathology and Surgery, Children's Hospital and Harvard Medical School, Boston, Massachusetts, USA;* [2]*Physiology Program, Harvard School of Public Health, Boston, Massachusetts, USA*

Received 31 March 2003; accepted in revised form 29 May 2003

Key words: cell cycle, cytoskeleton, extracellular matrix, mechanical force, microfilament, tension

Abstract

Caldesmon (CaD), a protein component of the actomyosin filament apparatus, modulates cell shape and cytoskeletal structure when overexpressed. When capillary endothelial cells were infected with an adenoviral vector encoding GFP-CaD under Tet-Off control, progressive inhibition of contractility, loss of actin stress fibers, disassembly of focal adhesions, and cell retraction resulted. This was accompanied by a cell shape (rounding)-dependent increase in apoptosis and concomitant inhibition of cell cycle progression. Cell growth also was inhibited in low expressor cells in which cell tension was suppressed independently of significant changes in cell shape, cytoskeletal structure, or focal adhesions. Thus, changes in both cytoskeletal structure and contractility appear to be central to the mechanism by which extracellular matrix-dependent changes in capillary cell shape influence growth and apoptosis during angiogenesis, and hence the cytoskeleton may represent a potential target for anti-angiogenesis therapy.

Introduction

Capillary endothelial (CE) cells control their ability to switch between different fates, including growth, apoptosis, differentiation, and motility, through adhesive interactions with extracellular matrix (ECM) (reviewed in [1]). The ECM exerts these effects, in part, based on its ability to resist cell tractional forces and thereby promote alterations in cell shape [2–7]. For example, CE cells proliferate on ECM substrates that permit cell spreading, whereas the same growth factor-stimulated cells switch off growth and undergo apoptosis when cultured on identically coated substrates that restrict cell extension [5]. CE cell cycle progression can be similarly inhibited by treating cells with pharmacological agents that disrupt the actin cytoskeleton (CSK), such as cytochalasin D (CytoD) or latrunculin B, or with drugs that inhibit cytoskeletal tension generation (e.g., 2,3-butanedione 2-monoxime; BDM) [6]. Treatment of cells with CytoD or with nocodazole to depolymerize the microtubule system also promotes apoptosis in these cells *in vitro* [8] and ECM dissolution results in both CE cell retraction and capillary involution *in vivo* [2, 9]. Many other studies also have shown that cell growth and apoptosis can be modulated by drugs that modify cytoskeletal structure in various cell types [6, 10–14]. However, the results of studies with pharmacological modifiers may be complicated by potential side effects of these chemical agents.

We therefore used a genetic approach to modulate cell shape and contractility, and to analyze the mechanism by which these variables switch CE cells between growth and apoptosis. Past investigators have shown that transfection of cells with high levels of a green fluorescent protein (GFP)-labeled form of non-muscle caldesmon (CaD), a protein component of the contractile actomyosin filament apparatus, results in disruption of focal adhesions, loss of actin stress fibers, and cell retraction in cultured fibroblasts [15, 16]. CaD was originally found in smooth muscle cells in the gizzard [17]. It is found within the contractile apparatus and binds to its various component proteins, including actin, myosin, tropomyosin, and calmodulin; its function is also under control of calcium/calmodulin interactions [18, 19]. When CaD binds to actin, it inhibits the ATPase activity of actomyosin in a calcium- and

Correspondence to: Donald E. Ingber, Vascular Biology Program, Departments of Surgery and Pathology, Children's Hospital and Harvard Medical School, Enders 1007, 300 Longwood Avenue, Boston, MA 02115, USA. Tel: +1-617-355-8031; Fax: +1-417-730-0230; E-mail: donald.ingber@tch.harvard.edu

calmodulin-dependent manner [20, 21] and thereby inhibits formation of both actin fiber bundles and focal adhesions [15].

Past studies used plasmid-based vectors to constitutively express GFP-CaD in fibroblasts [15, 16]. In contrast, in the present study, we used an adenovirus-mediated expression system under control of a tetracycline (Tet)-inducer (AdTet-Off) to achieve efficient, synchronous, and tunable expression of CaD-GFP in CE cells. This allowed us to unequivocally address the question: does the actin CSK actively regulate switching between growth and apoptosis in CE cells?

Materials and methods

Experimental system

Bovine CE cells were isolated and cultured on gelatin-coated dishes as described (9). Cells were cultured in DMEM supplemented with 10% fetal bovine serum (FBS; Clonetics/BioWhitaker, San Diego, California), 2 mM glutamine, 100 U/ml penicillin, 100 U/ml streptmycin (Invitrogen/GIBCO, Carlsbad, California), and 5 ng/ml basic fibroblast growth factor (Biomedical Technologies Inc., Stoughton, Massachusetts), unless otherwise indicated. We used the Tet-Off expression system developed by Gossen et al. [22, 23] to deliver tetracycline-regulated expression based on the high specificity of the *Escherichia coli tet* repressor-operator-tetracycline interaction. Induction of expression of the integrated target gene is controled solely by removing Tet from the culture medium.

In our studies, the plasmid of GFP-tagged cDNA containing the full-length rat non-muscle CaD gene (kindly supplied by Dr David M. Helfman, Cold Spring Harbor Laboratory) was used as the template plasmid. The shuttle vector plasmid pTRE2-shuttle containing the minimal cytomegalovirus promoter and *tet*-operator sequences cloned upstream of the cDNA to be expressed and the Tet-Off system were purchased from BD Biosciences Clontech (Palo Alto, California). The GFP-CaD gene was excised from the template plasmid at Xba I (5′) and BamHI (3′) restriction sites, both intruding ends were blunted with a DNA blunting kit (TAKARA, Japan) and then ligated at the EcoRV site of the pTRE2-shuttle vector. The orientation of the insert was verified by restriction analysis. Human kidney-derived 293 epithelial cells were obtained from QBIOgene (Carlsbad, California) and cultured in 25 cm^2 flasks in 10%FBS/DMEM to a subconfluent density prior to transfection. The pTRE2 shuttle vector containing GFP-CaD gene was ligated with the adenoviral genome DNA (provided by Clontech) and transfected into the 293 cells diluted in Optimem (Invitrogen/Life Technologies, Carlsbad, California) with lipotransfection reagent, LipofectAMINE 2000 (Invitrogen/Life Technologies, Carlsbad, California). After 2 or 3 days, cells became round and detached from the substrate due to the cytopathic effect of the adenoviral infection and floated in the medium until 7 days after transfection. The cells were then collected in a tube, repeatedly frozen and thawed 5 times, and collected by centrifugation (1500 rpm). The supernatants containing recombinant adenovirus particles encoding GFP-caldesmon (AdGFP-CaD; first seed) were aliquoted and stored at −80 °C. To obtain higher titers of the adenoviral vectors, this process was repeated two additional times. The final (third) round produced viral titers ranging from 10^9 to 10^{10} pfu/ml, as determined by plaque assay in 293 cells. The presence of the cDNA insert was confirmed by direct observation of actin fiber disruption within the cells transfected with AdGFP-CaD and AdTet-Off in Tet-free medium, and by Western blot analysis of cell lysates.

Analysis of switching between growth and apoptosis

Progression of quiescent CE cells through the cell cycle and into S phase was measured by quantitating the percentage of cells that exhibited nuclear incorporation of bromo-2′deoxyuridine (BrdU) after continuous exposure for 24 h, as previously described [6]. One day after cells were plated, the DMEM/10%FBS was replaced 0.4% FBS/DMEM containing 10^8 pfu/ml of AdGFP-CaD and AdTet-Off and 10 μg/ml of Tet; cells were then cultured for 36–48 additional hours. As previously demonstrated [24], CE cells synchronize in G_0 when maintained in low serum for 2–3 days in culture. GFP-CaD expression was induced these quiescent cells by culturing the cells in the same low serum medium without Tet for 24 additional hours. At that time, cells were induced to reenter into the cell cycle by replacing the medium with 10% FBS/DMEM containing BrdU, in the continued absence of Tet. Control cultures were treated identically except that Tet was maintained in the medium throughout the entire experiment.

Cells were fixed 24 h after cell cycle release in 5% acetic acid/90% ethanol for 30 min at room temperature. BrdU positive cells were identified by incubating cells with anti-BrdU antibody and nuclease (RPN202, Amersham Biosciences) for 60 min, and stained with biotinylated anti-mouse Ig antibodies and Texas red-avidin (Vector Laboratories, Burlingame, California). BrdU-positive cells were visualized and scored using a Nikon epifluorescence microscope with 20× objectives; all nuclei were counter-stained with the DNA binding dye, 4,6-diamino-2-phenylindole (DAPI, 1 μg/ml). Cells were analyzed in 12 random fields from duplicates in at last three experiments; the data presented represent results from more than 200 cells for each data point. To determine the precise relationship between GFP-CaD expression, DNA synthesis, apoptosis and cell spreading, CE cells were divided into following subgroups based on projected cell areas measured using computerized image analysis: <1000, 1000–2000, 2000–3000, and >3000 μm^2. The data presented represent the mean

values ± standard error for all parameters (GFP intensity, TUNEL staining, BrDU incorporation) within each of these subgroups.

To measure effects on apoptosis under similar conditions, CE cells were fixed with 4% paraformaldehyde/PBS for 15 min at room temperature in parallel studies. To detect apoptosis, cells were permeabilized with 0.1% sodium citrate/0.1% Triton-X 100 in PBS, and stained with terminal deoxynucleotidyl transferase dUTP nick-end labeling (TUNEL) enzyme reagent (*In situ* Cell Death Detection kit; Roche Molecular Biochemicals, Indianapolis, Indiana). The apoptosis index was calculated as the percentage of DAPI-labeled nuclei that exhibited positive TUNEL staining as detected using fluorescence microscopy as previously described [6, 8].

Immunocytochemistry and computerized image analysis

For immunocytochemistry, CE cells cultured on 35 mm dishes with thin glass bottoms (MatTek, Ashland, Massachusetts) were fixed in 4% paraformaldehyde/PBS for 15 min at room temperature. To visualized actin microfilaments, cells were incubated with fluorochrome conjugated-phalloidin (Alexa Flour™ 594 Phalloidin, Molecular Probes, Eugene, Oregon) for 30 min, washed with PBS and mounted with FluoromoutG compound (Southern Biotechnology Associates, Inc., Birmingham, Alabama). For localization of focal adhesions, cells were incubated with anti-human paxillin antibodies (Transduction Laboratories, Lexington, Kentucky) and stained with biotinylated anti-mouse Ig antibodies and Texas red-avidin with DAPI counterstaining. Projected cell areas and average GFP intensity of each cell (depicted as pixel intensity/μm^2) were determined from digitized images using IPlab Spectrum and RatioPlus, image analysis and microfluorimetry software (Scanalytics, Inc, Fairfax, Virginia), as previously described [7].

Cell contractility measurements

The tractional stresses exerted by individual cultured CE cells were quantitated using a modified form of traction force microscopy, as previously described [25]. Briefly, BCE cells were transfected with AdGFP-CaD and AdTet-Off (10^8 pfu each for CE cells in 35 mm dishes), incubated for 2 days in the presence of Tet, and then replated in 0.4% FBS/DMEM on flexible polyacrylamide gel substrates (Young's moduli of 1300 or 4000 Pa) coated with fibronectin (50 ng/cm^2) that contained red-fluorescent nanobeads (200 nm diameter; Molecular Probes) as fiducial markers. One day later, projected cell areas and mean GFP-staining intensity were measured. Nanobead positions were measured before and after trypsin or warm 10% SDS was added to the cultures to detach the cells (similar results were obtained with both techniques, although the SDS provided more rapid cell detachment). Isometric tension forces exerted by each of the adherent cells were determined by comparing bead position before and after cell detachment and calculating relative bead displacements.

Statistical analysis

All data are presented as mean ± standard error. For comparison of GFP intensities between control and GFP-CaD expressor cells, a Student's *t*-test was performed. A polynominal regression was performed to compare the relationship between GFP intensities and projected cell areas in Figure 4.

Results

Tet-dependent control of GFP-CaD expression

CE cells transfected with AdTet-Off and AdGFP-CaD in the presence of Tet did not show any detectable GFP expression. In contrast, GFP-CaD positive cells appeared within 6 h after removal of Tet from the medium (Figures 1A, C), and virtually all of the cells expressed the transgene by 48 h (Figures 1B, D). Quantitation of the percentage of GFP-positive cells confirmed that the transgene was induced within hours after Tet removal, with over 97% of cells staining positively for GFP-CaD by 24–48 h (Figure 1E). Thus, the Ad Tet-Off system provides a highly efficient method for synchronous activation of GFP-CaD in cultured CE cells.

Effects of CaD on cell shape, the actin cytoskeleton, and focal adhesions

Induction of GFP-CaD expression by removal of Tet resulted in significant changes of cell shape and cytoskeletal structure over time. When analyzed at 6 h after Tet removal, GFP-CaD colocalized with F-actin within well spread cells, as detected by staining with Alexa Flour™ 594-phalloidin (Figure 2), and with well developed, paxillin-containing focal adhesions that appeared at the ends of each actin bundle (Figure 3). Analysis of cells in Tet-free medium over time, revealed that continued transgene expression resulted in progressive disassembly of actin bundles, such that only occasional small filaments that contained both F-actin and GFP-CaD could be observed by 12 h. Partial disruption of the actin CSK also was accompanied by focal adhesion disassembly (Figure 3) and loss of cell extensions, such that although the cells remained adherent, they exhibited more polygonal forms (Figure 2). By 24 h, complete loss of filamentous actin (Figure 2) and focal adhesions (Figure 3) was observed and cells exhibited fully retracted, dendritic forms that were highly reminiscent of CE cells treated with Cyto D [26]. Quantitation of changes in GFP-CaD intensities in cells cultured for various times confirmed that there was a tight correlation ($R^2 = 0.89$, $P < 0.001$) between GFP-CaD expression levels and the degree of cell spreading, as measured by quantitating projected cell areas using computerized

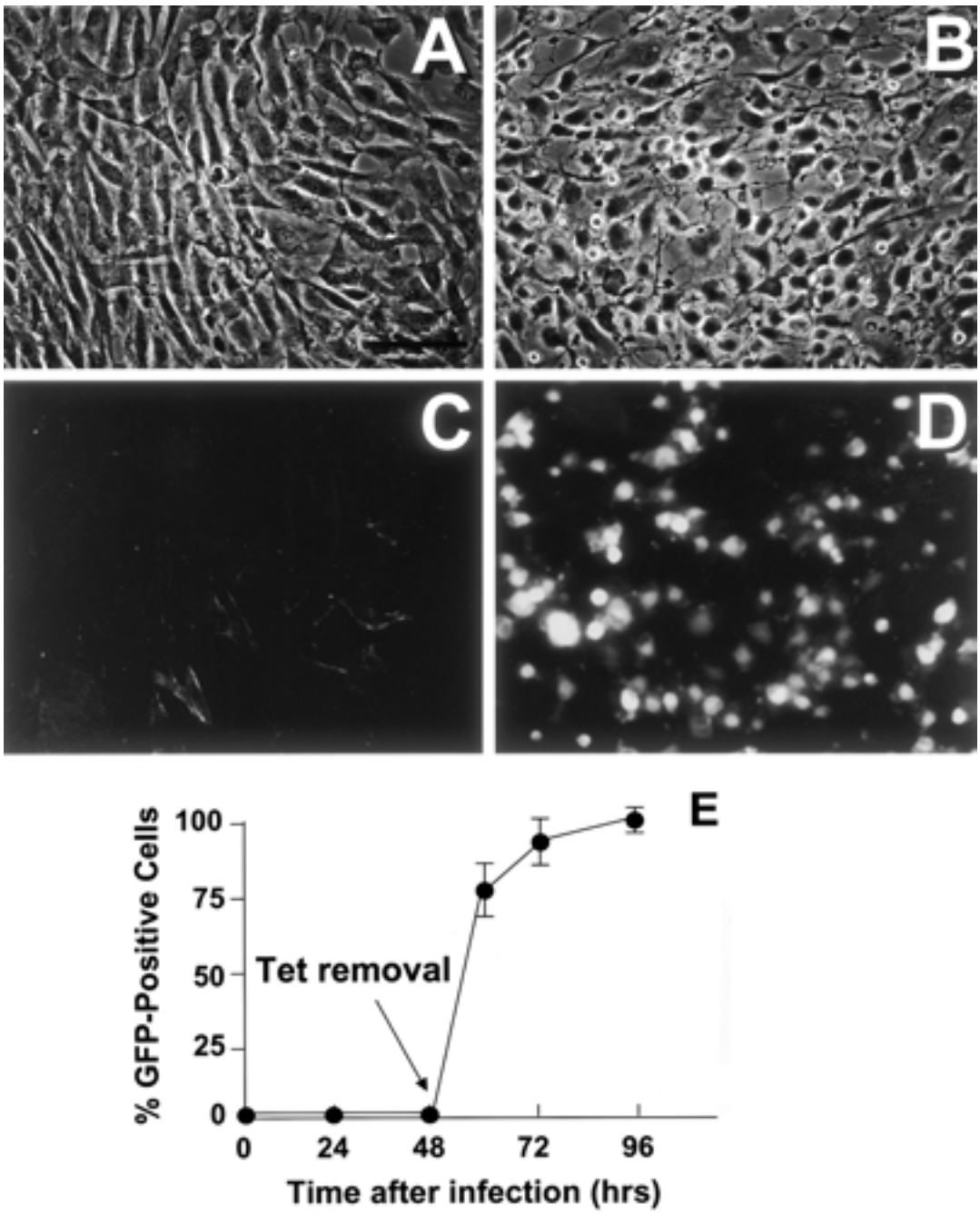

Figure 1. Regulated control of GFP-CaD expression by the adenovirus-mediated Tet-Off system. Phase contrast (A, B) and fluorescent (C, D) images of CE cells that were transfected with AdGFP-CaD and AdTet-Off, 6 h (A, C) or 48 h (B, D) after Tet was removed from the medium. Note that GFP-CaD expression was detectable within actin stress fibers in spread cells as early as 6 h after Tet removal and that cells retracted and rounded by 48 h (bar = 250 μm). (E) Quantitation of the efficiency of transgene expresssion by measuring the percentage of GFP-positive cells.

image analysis (Figure 4). The highest GFP expressing cells had projected areas of about one-seventh that of control cells.

Effects on cell contractility

The past finding that overexpression of GFP-CaD by transient transfection produced similar effects on cell morphology suggested that GFP-CaD might interfere directly with actomyosin-based tension generation in non-muscle cells [15, 27] as it does in muscle [21]. To definitively address this question, we quantitated cell contractility in CE cells expressing GFP-CaD using traction force microscopy [25, 28]. In this method, cells are cultured on flexible, ECM-coated, polyacrylamide substrates that contain fluorescent nanobeads embedded beneath the surface of the gels. By measuring the displacement of the beads before and after detachment of the cells, it is possible to quantitate the isometric tensional forces or traction that the cells exert on the substrate [25, 28, 29]. Cells expressing GFP-CaD displayed fewer and less intense regions of high stress in

their underlying substrate, even at the lowest level of GFP-CaD expression (Figure 5A). Quantitation of the levels of tractional stress exerted by cells expressing different levels of GFP-CaD 16–28 h after Tet removal, revealed that cell traction progressively decreased with increasing GFP-CaD levels, which again was paralleled by decreases in cell spreading (Figure 5B). The most-rounded cells showed about one-tenth the level of traction exhibited by control cells. Importantly, the cells that exhibited the lowest level of GFP-CaD expression displayed a major decrease (>50%) in cell contractility relative to controls on these flexible substrates ($P < 0.01$, Figure 5B), even though there was no significant change in projected cell area ($P = 0.09$). Cells that displayed the lowest level of GFP-CaD expression did not display any obvious alteration in the appearance of their stress fibers or focal adhesions which appeared nearly identical to those observed in cells 6 h after Tet removal (Figures 2 and 3).

CaD-dependent switching between apoptosis and growth

To explore the effects of CaD expression on cell apoptosis and growth, cells were refed with low serum (quiescence) medium without Tet to induce GFP-CaD expression for 24 h before cells were stimulated to reenter the cell cycle by addition of high serum. The apoptosis rate detected by nuclear TUNEL staining progressively increased after cell cycle reentry in parallel with the level of GFP-CaD expression, with over 35% of the highest expressor cells exhibiting positive TUNEL staining within 24 h after serum addition. In contrast, control cells maintained in the continuous presence of Tet did not change their apoptosis labeling index which remained constant at 6%–8% throughout the entire study period. To more accurately determine the relationship between cell shape, apoptosis and CaD expression, we quantitated nuclear TUNEL staining, projected cell areas and GFP staining intensity in cells that exhibited different levels of GFP-CaD expression 24 h after release into the cell cycle. The percentage of apoptotic cells progressively increased more than 4-fold as GFP intensity increased (Figure 6A) and cell retraction was promoted (Figure 6B). The lowest level of GFP-CaD expression that was sufficient to reduce cell contractility but not cell spreading (Figure 5), exhibited low levels of apoptosis that were not significantly different from non-infected controls (Figure 6B).

CE cell entry to S phase was also measured in cells cultured under the same conditions by quantitating BrdU incorporation into nuclei. CE cells that were infected with the adenoviral vectors but maintained in the presence of Tet to suppress GFP-CaD expression progressed normally through the cell cycle and exhibited a DNA labeling index of approximately 40%. In contrast, progressive increases in the expression of GFP-CaD that promoted apoptosis also produced concomitant inhibition of growth (Figure 6A). Again, inhibition of DNA synthesis correlated closely with effects on cell spreading, however, the cells expressing the lowest level of GFP-CaD exhibited a small, but statistically significant inhibition of growth compared to controls ($P < 0.05$, Figure 6B), in the absence of a significant change in cell shape (Figure 5B). In separate studies, similar expression of a truncated form of GFP-caldesmon (AA 237–445) that was previously shown to be inactive in terms of altering cell shape or focal adhesion formation [15] did not produce apoptosis or inhibit growth (not shown).

Discussion

The CE cell's ability to switch between growth, apoptosis, and differentiation in the local tissue microenvironment during angiogenesis is controled through cell interactions with the ECM [1]. The ECM exerts these effects, in part, by altering cell shape [3, 5, 24]. Past studies have shown, for example, that individual CE cells progress through the cell cycle when they are allowed to adhere and extend over large ECM islands (>50 μm diameter circles), whereas cells adherent to smaller ECM islands (<20 μm) that prevent cell spreading undergo apoptosis despite the presence of mitogenic factors [5]. CE cells also remain viable and proliferate when cultured on multiple smaller (3–5 μm) ECM islands that are more closely positioned so that they promote cell spreading, even though they form the same total area of cell-ECM contact as on a single small apoptosis-inducing island [5]. Thus, these results suggested that cell spreading *per se* may be a critical governor of cell growth and viability. Later studies revealed that the effects of cell shape on cell proliferation and apoptosis are mediated through the CSK in CE cells. Disruption of actin microfilaments using CytoD or latrunculin, or inhibition of cytoskeletal tension generation using BDM, produced a similar cell cycle block in G1 as cell rounding [6]. Both actin microfilament disruption and depolymerization of microtubules using nocodazole also induced apoptosis in the presence of growth factors and ECM adhesion in CE cells [8]. Moreover, similar effects of cytoskeletal-modifying drugs have been observed in many cell types and experimental systems [6, 10–13]. However, the results of studies with pharmacological modifiers can be complicated by potential side effects of these chemical agents [30]. Thus, here we used a genetic technique to manipulate cytoskeletal structure and tension generation to unambiguously determine whether these structural cues are critical regulators of cell fate switching in CE cells.

To directly determine whether the CSK is an active control element in CE cells, we engineered adenoviral vectors encoding GFP-CaD and a Tet-Off inducible promoter. When cultured CE cells were infected with these vectors, synchronous and highly efficient (>97%) expression of GFP-CaD was produced. Increases in the intensity of GFP-CaD expression measured using microfluorimetry resulted in progressive disruption of actin

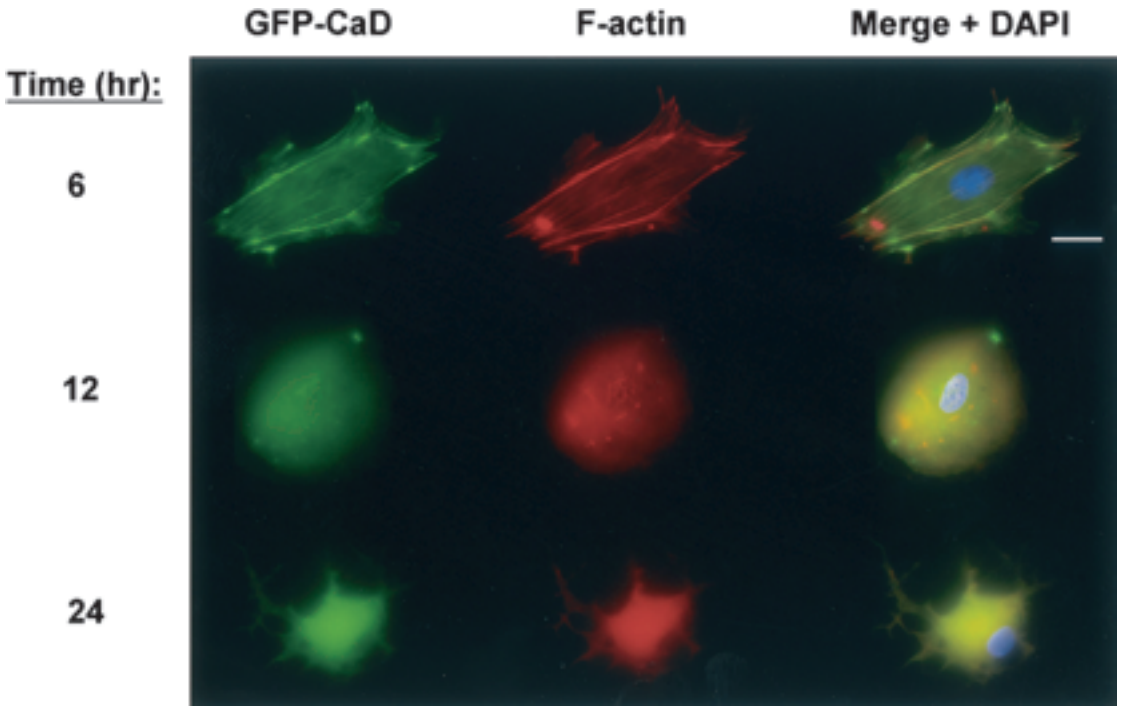

Figure 2. Disruption of the actin cytoskeleton by expression of GFP-CaD. CE cells were transfected with AdGFP-CaD and AdTet-Off and cultured for 6 (top), 12 (middle) or 24 (bottom) hrs in the absence of Tet. GFP-CaD, F-actin (stained with Alexa Fluor 594-phalloidin) and DAPI-stained nuclei within cells that exhibited various levels of GFP-CaD expression after Tet removal were visualized by fluorescence microscopy. (Top) GFP-CaD localized within actin microfilament bundles within well spread cells when expressed for 6 h (Middle) Cells that expressed GFP-CaD for longer time (12 h) lacked well developed stress fibers and exhibited a more polygonal shape. Note that a few small residual actin fibers remain in the supranuclear region. (Bottom) After 24 h, GFP-CaD expressing cells exhibited highly retracted, dendritic forms and complete loss of detectable filamentous actin.

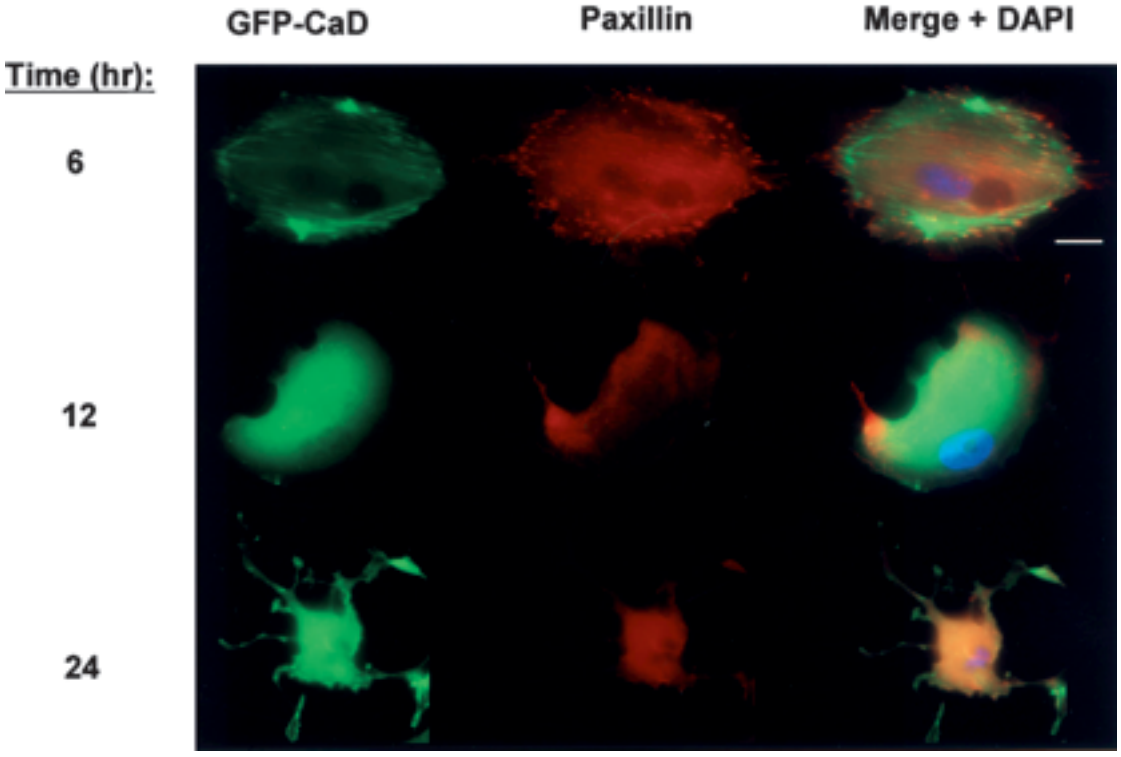

Figure 3. GFP-CaD overexpression induces focal adhesion disassembly. Cells were processed as in Figure 2 except that focal adhesions were visualized by staining cells with anti-paxillin antibodies. *Top*: paxillin-containing focal adhesions colocalized with the ends of actin bundles that also co-stained with GFP-CaD at 6 h after transgene induction. *Middle*: at 12 h, most focal adhesions had disassembled and only rare small, punctate, paxillin-staining adhesion sites remained. *Bottom*: complete loss of focal adhesions was observed after 24 h of culture in the absence of Tet.

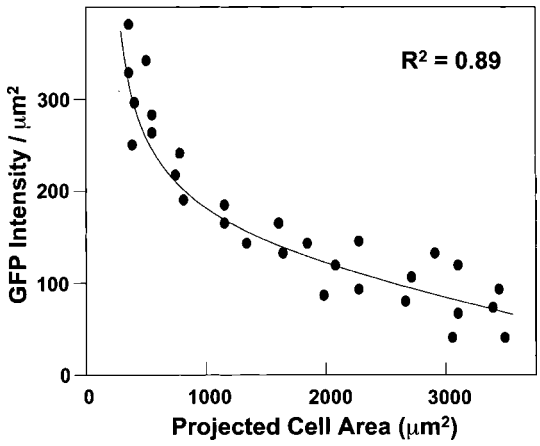

Figure 4. Quantitation of the relation between GFP staining intensity and cell shape. Projected cell areas were determined using computerized image analysis; GFP-CaD intensities was measured within the same cells using computerized microfluorimetry and normalized for cell size (GFP intensity/μm^2). Polynominal regression showed a close inverse relationship between GFP-CaD intensity and projected cell area ($R^2 = 0.89$, $P < 0.001$).

stress fibers, disassembly of focal adhesions, and decreases in cell size. Similar effects were observed in past studies in which GFP-CaD was transiently transfected into fibroblasts, except that the efficiency of transgene expression was low and there was no control over the timing of expression [15]. In contrast to those past studies, we also observed highly retracted cells with dendritic appearance, reminiscent of CytoD-treated CE cells at the highest level of GFP-CaD expression, suggesting greater efficiency of the adenoviral approach.

Although the effects of GFP-CaD overexpression on the CSK and cell shape were thought to have resulted from inhibition of cytoskeletal tension generation in the past [15], a direct quantitative relationship between GFP-CaD levels and cytoskeletal tensional forces has never been demonstrated directly. In the present study, cell contractility was measured within individual cells using traction force microscopy and GFP-CaD expression levels were simultaneously quantitated in the same cells using microfluorimetry. These studies confirmed that increases in the GFP-CaD expression were accompanied by a progressive inhibition of cell traction (i.e., suppression of cell tension generation). Importantly, we found that inhibition of cell contractility is one of the earliest effects of GFP-CaD overexpression (i.e., it is observed at the lowest levels of GFP-CaD expression), and that it precedes changes in actin filament reorganization, focal adhesion assembly, or cell size. This finding suggests that small amounts of GFP-CaD that integrate into existing contactile microfilaments first interfere with tension generation through direct inhibition of the myosin ATPase. As more GFP-caldesmon molecules bind to the contractile apparatus, disassembly of microfilament bundles ensues, ultimately leading to cell retraction.

Why does increased GFP-CaD expression and loss of contractility (i.e., cytoskeletal tension generation) lead to collapse of the actin CSK and cell rounding? Cells normally experience isomeric tension (prestress) in their CSK that stabilizes cell shape and determines their mechanical properties [29, 31–34]. A force balance is maintained because cells are anchored *via* focal adhesions to the ECM which resists cell tractional forces. For cells to spread, they must generate forces great enough to overcome the mechanical stiffness of their entire CSK. Deformation of the cell and CSK is thus made possible because the rigidity of the ECM that resists cell-generated tractional forces allows the cell to progressively increase isometric tension inside the cell. As shown when mechanical forces are applied to integrins *via* bound ECM ligands, tension promotes focal adhesion formation and alignment of individual cytoskeletal filaments into larger filament bundles (i.e., stress fiber assembly); this results in an increase in both anchoring strength and mechanical stiffness of the cell until the forces come into balance and cell shape is stabilized [31, 35–40]. Thus, over expression of CaD will first begin to destabilize the cell mechanics by decreasing CSK prestress and by promoting CSK filament bundles to disassemble into individual contractile microfilaments. Tension inhibition also leads to focal adhesion disassembly [15, 38]. In fact, the number of stress fibers and focal adhesions both decrease when cell tension is inhibited using BDM to chemically interfere with myosin ATPase activity [6, 39], much as they did when GFP-CaD was overexpressed in the present study. Increased levels of CaD also will lead to progressive disruption of the individual contractile microfilaments through competitive binding for components of the contractile apparatus (e.g., actin, myosin, tropomyosin, calmodulin); in this manner, complete loss of CSK shape stability results leading to cell retraction due to residual surface membrane tension. CaD may therefore cause cell retraction because it breaks the self-stabilizing force-balance that normally maintains the mechanical stiffness of the entire actin CSK as well as the structural stability of individual focal adhesions.

Importantly, these genetically induced changes in cytoskeletal structure and contractility had potent effects on CE cell function. In particular, the cells were switched from growth to apoptotic programs by expressing increasing levels of GFP-CaD. Growth decreased and apoptosis increased as GFP-CaD intensity levels rose and cell retraction was promoted. These results confirm past findings which demonstrated that CE cells can be similarly switched from growth to quiescence, and eventually to apoptosis, by preventing cell spreading using standard culture substrates overlaid with non-adhesive polymers [41], small micropatterned ECM adhesive islands [5], or by disrupting the actin CSK using chemical agents [7]. It is possible that overexpression of caldesmon could trigger apoptosis by directly altering components of the cytoskeleton-associated apoptotic machinery (i.e., independently of higher order structural changes). However, we believe this unlikely given that we have obtained nearly identical effects on the apoptotic signaling pathway (e.g., Akt,

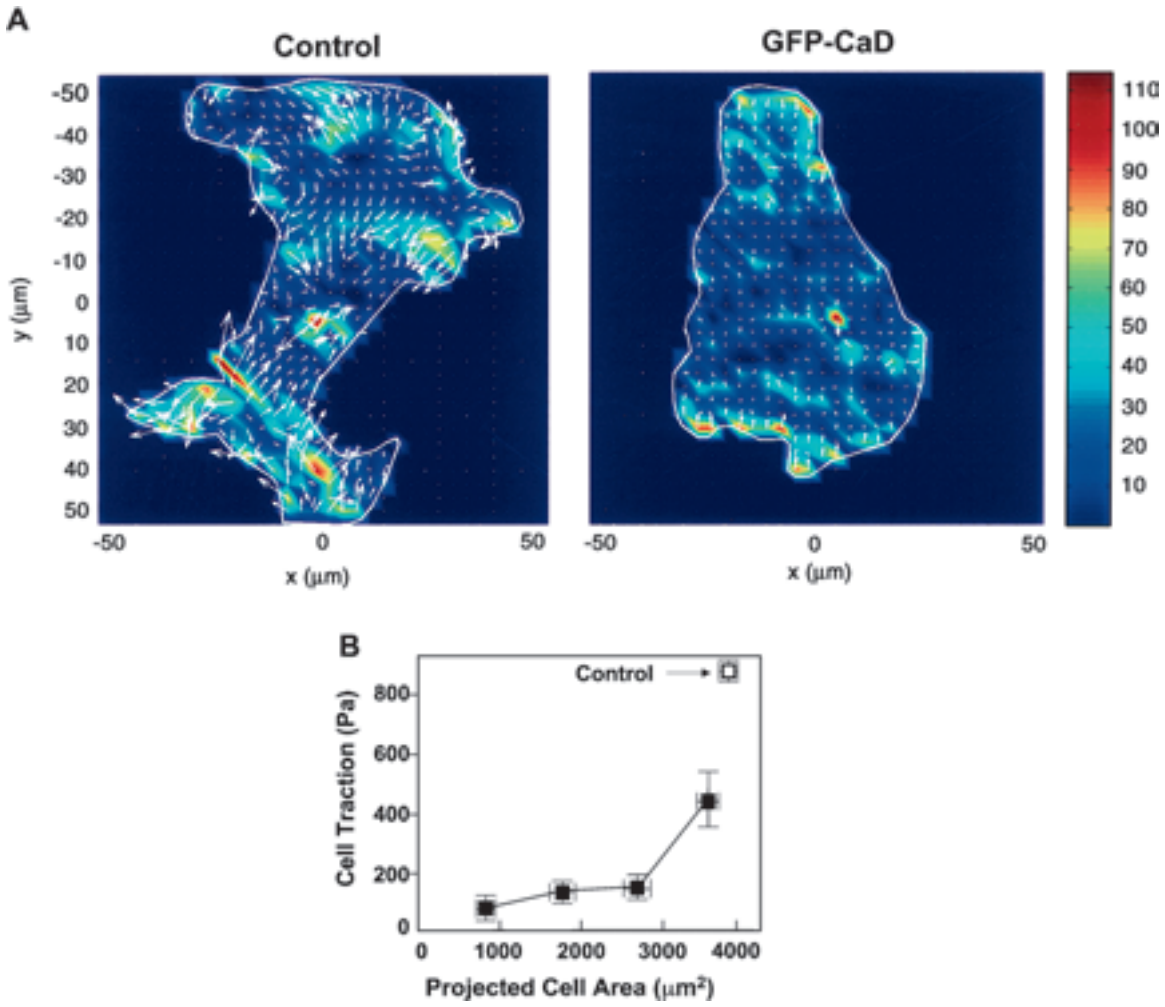

Figure 5. Quantitation of the effects of GFP-CaD expression on cell contractility. (A) Maps of the traction fields of control cells (left) and cells expressing low levels of GFP-CaD 24 h after Tet removal (right), as generated by tractional force microscopy. Arrows indicate direction of bead displacements and associated traction stresses. The color scale indicates magnitudes of the tractions (in Pa); red and orange regions indicate areas of highest concentration of traction. (B) Plot of cell traction as a function of projected cell area. Black squares, cells expressing different GFP-CaD expression levels (from left to right: 203 ± 23, 125 ± 18, 85.9 ± 19, 52.1 ± 17/μm^2); open square, control cells. Note that cells which express the lowest level of GFP-CaD and only exhibit a minimal change in cell area display a major decrease in cell contractility.

bcl-2) with direct modulators of cytoskeletal integrity (e.g., cytochalasin D) [8]. Interestingly, inhibition of cell contractility in low GFP-CaD expressor cells that maintained normal cell shape did not trigger apoptosis, although it blocked cell cycle G1 progression. This is consistent with the finding that while inhibition of cytoskeletal tension generation with BDM prevents cell cycle progression [6], it has no effect on programmed death in these CE cells [7]. Thus, cell growth appears to be more sensitive to changes in cytoskeletal tension than apoptosis.

It is important to note that proliferation was inhibited in the low GFP-CaD expressor cells that exhibited a major decrease in contractility, even though there was no detectable change in cell shape, stress fibers, or focal adhesions. This finding confirms that suppression of cell tension (CSK prestress) has a direct effect on cell cycle progression, independently of cell shape or changes in CSK integrity, as previously proposed [6]. Caldesmon has been shown to be a target for p38MAPK [42] and thus over-expression of this substrate could feed back to directly alter this growth signaling pathway. However, again we believe this unlikely for multiple reasons: (1) entirely different chemical agents that directly modulate cytoskeletal integrity or tension generation produce nearly identical effects [6, 14], (2) GFP-caldesmon's dose–dependent growth effects in the present study correlated directly with its effects on cell shape and cytoskeletal organization, and (3) the shape-dependent cell cycle restriction point functions independently of MAPK signaling in endothelial cells [14].

Thus, the major determinant of both cell cycle progression and the switch to apoptosis in capillary cells appears to be large-scale alterations in the structural state of the actin CSK that produce global changes in cell shape. This finding may be of general interest because pharmacological disruption of the actin CSK that causes cell retraction also inhibits cell growth and induces apoptosis in many other cell systems [10–13]. These results also provide additional support for the

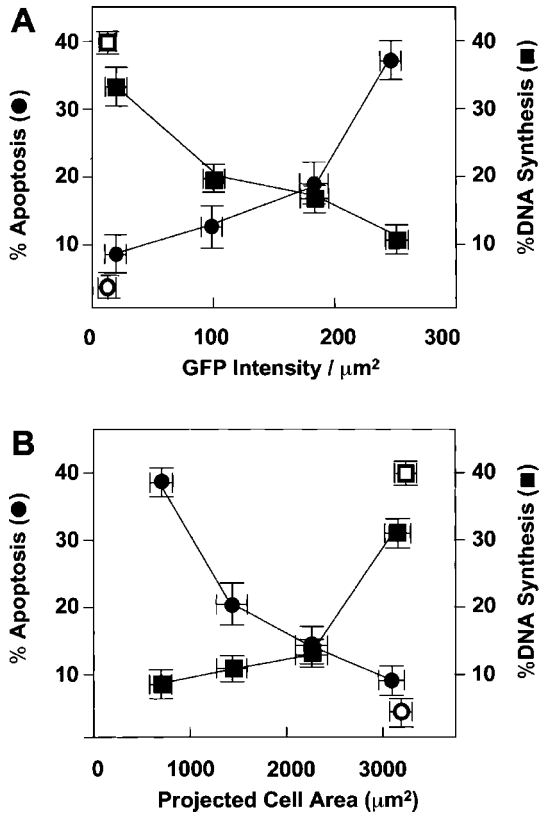

Figure 6. GFP-CaD regulates switching between cell growth and apoptosis. Apoptosis and DNA synthesis indices in CE cells shown as a function of GFP-CaD staining intensity (A) and projected cell area (B). Circles, % cells with TUNEL-positive apoptotic nuclei; Squares, % cells with BrdU-positive nuclei that entered S phase; black symbols, GFP-CaD-expressing cells; white symbols, control cells.

concept that local ECM-dependent changes in cell shape or in the mechanical context of a cell may govern its response to soluble modulators during tissue morphogenesis [1, 43]. In fact, in the case of angiogenesis, capillary sprout elongation can be stimulated by direct application of tensional forces in three-dimensional cultures [44], and drugs that cause ECM breakdown and promote CE cell retraction induce cell death and capillary involution *in vivo* [2, 9]. Transcriptional changes in the level of endogenous caldesmon protein also accompany capillary differentiation (tube formation) *in vitro* [45], adding further support for the concept that the CSK represents a physiological target for angiogenic control. Studies with mammary glands maintained in three-dimensional cultures similarly show that the physical tissue context is a key determinant of apoptosis sensitivity to chemotherapeutic agents and immune modulators as well as cell differentiation [46–48]. Branching morphogenesis also can be controled by altering CSK tension in embryonic lung [49]. Thus, the critical role that the CSK plays in developmental control may be based on its ability to locally modulate cell fate switching in a tissue microenvironment that contains various soluble regulatory stimuli.

The adenovirus-mediated, inducible expression system used here enabled us to tightly control target gene expression with maximal transgene efficiency in CE cells. Adenoviral Tet-regulatable systems also have been shown to be suited for use in animals [50]. This novel system could facilitate functional studies of cell contractility or exploration of new therapeutic approaches within the context of whole tissues where cell fate regulation by changes in CSK structure or tension may be crucial for tissue morphogenesis [43, 49]. Moreover, the finding that a specific component of the actomyosin contractile apparatus – caldesmon – provides such fine control over cell fate switching in CE cells raises the possibility that molecules that are involved in the cell contractility pathway might represent potential targets for therapeutic intervention in angiogenesis-dependent diseases, such as cancer and rheumatoid arthritis.

Acknowledgements

We would like to thank J. Chen and S. Hu for their technical assistance, S. Huang for reviewing the manuscript, and NIH (CA55833 and CA45548 to DEI) and NASA (NAG2-1509 to NW) for their grant support.

References

1. Ingber DE. Mechanical signaling and the cellular response to extracellular matrix in angiogenesis and cardiovascular physiology. Circ Res 2002; 91: 877–87.
2. Ingber DE, Madri JA, Folkman J. A possible mechanism for inhibition of angiogenesis by angiostatic steroids: Induction of capillary basement membrane dissolution. Endocrinology 1986; 119: 1768–75.
3. Ingber DE, Folkman J. How does extracellular matrix control capillary morphogenesis? Cell 1989; 58: 803–5.
4. Singhvi R, Kumar A, Lopez GP et al. Engineering cell shape and function. Science 1994; 264: 696–8.
5. Chen CS, Mrksich M, Huang S et al. Geometric control of cell life and death. Science 1997; 276: 1425–8.
6. Huang S, Chen CS, Ingber DE. Control of Cyclin D1, $p27^{kip1}$, and cell cycle progression in human capillary endothelial cells by cell shape and cytoskeletal tension. Mol Biol Cell 1998; 9: 3179–293.
7. Parker KK, Brock AL, Brangwynne C et al. Directional control of lamellipodia extension by constructing cell shape and orienting cell tractional forces. FASEB J 2002; 16: 1195–204.
8. Flusberg DA, Numaguchi Y, Ingber DE. Cooperative control of Akt phopsphorylation, bcl-2 expression, and apoptosis by cytoskeletal microfilaments and microtubules in capillary endothelial cells. Mol Biol Cell 2001; 12: 3087–94.
9. Ingber DE, Folkman J. Inhibition of angiogenesis through inhibition of collagen metabolism. Lab Invest 1988; 59: 44–51.
10. Iwig M, Glaesser D, Bethge M. Cell shape-mediated growth control of lens epithelial cells grown in culture. Exp Cell Res 1981; 131: 47–55.
11. Sauman I, Berry SJ. Cytochalasin D treatment triggers premature apoptosis of insect ovarian follicle and nurse cells. Int J Dev Biol 1993; 37: 441–50.
12. Böhmer RM, Scharf E, Assoian RK. Cytoskeletal integrity is required throughout the mitogen stimulation phase of the cell cycle and mediates the anchorage-dependent expression of cyclin D1. Mol Biol Cell 1996; 7: 101–11.
13. Korichneva I, Hammerling U. F-actin as a functional target for retro-retinoids: A potential role in anhydroretinol-triggered cell death. J Cell Sci 1999; 112: 2521–8.

14. Huang S, Ingber DE. A discrete cell cycle checkpoint late G1 that is cytoskeleton-dependent and MAP kinase (Erk)-independent. Exp Cell Res 2002; 275: 255–64.
15. Helfman DM, Levy ET, Berthier C et al. Caldesmon inhibits nonmuscle cell contractility and interferes with the formation of focal adhesions. Mol Biol Cell 1999; 10: 3097–112.
16. Geiger B, Bershadsky A. Assembly and mechanosensory function of focal contacts. Curr Opin Cell Biol 2001; 5: 584–92.
17. Sobue K, Muramoto Y, Fujita M, Kakiuchi S. Purification of a calmodulin-binding protein from chicken gizzard that interacts with F-actin. Proc Natl Acad Sci USA 1981; 78: 5652–5.
18. Matsumura F, Yamashiro S. Caldesmon. Curr Opin Cell Biol 1993; 5: 70–6.
19. Huber PA. Caldesmon. Int J Biochem Cell Biol 1997; 29: 1047–51.
20. Marston SB, Fraser IDC, Huber PAJ et al. Location of two contact sites between human smooth muscle caldesmon and Ca^{2+}-calmodulin. J Biol Chem 1994; 269: 8134–9.
21. Chalovich JM, Sen A, Resetar A et al. Caldesmon: binding to actin and myosin and effects on elementary steps in the ATPase cycle. Acta Physiol Scand 1998; 164: 427–35.
22. Gossen M, Bujard H. Tight control of gene expression in mammalian cells by tetracycline-responsive promoters. Proc Natl Acad Sci USA 1992; 89: 5547–51.
23. Gossen M, Freundlieb S, Bender G et al. Transcriptional activation by tetracyclines in mammalian cells. Science 1995; 268: 1766–9.
24. Dike LE, Ingber DE. Integrin-dependent induction of early growth response genes in capillary endothelial cells. J Cell Sci 1996; 109: 2855–63.
25. Tolic-Norrelykke IM, Butler JP, Chen J, Wang N. Spatial and temporal traction response in human airway smooth muscle cells. Am J Physiol Cell Physiol 2002; 283: C1254–66.
26. Ingber DE, Prusty D, Sun Z et al. Cell shape, cytoskeletal mechanics, and cell cycle control in angiogenesis. J Biomech 1995; 28: 1471–84.
27. Pawlak G, Helfman DM. Cytoskeletal changes in cell transformation and tumorgenesis. Curr Opin Gen Dev 2001; 11: 41–7.
28. Pelham RJ Jr, Wang Y. High resolution detection of mechanical forces exerted by locomoting fibroblasts on the substrate. Mol Biol Cell 1999; 10: 935–45.
29. Wang N, Naruse K, Stamenovic D et al. Mechanical behavior of living cells consistent with the tensegrity model. Proc Natl Acad Sci USA 2001; 98: 7765–70.
30. Rubtsova SN, Kondratov RV, Kopnin PB et al. Disruption of actin microfilaments by cytochalasin D leads to activation of p53. FEBS Lett 1998; 430: 353–7.
31. Ingber DE. Cellular tensegrity: Defining new rules of biological design that govern the cytoskeleton. J Cell Sci 1993; 104: 613–27.
32. Wang N, Ingber DE. Control of cytoskeletal mechanics by extracellular matrix, cell shape, and mechanical tension. Biophys J 1994; 66: 1281–9.
33. Wang N, Ostuni E, Whitesides GM, Ingber DE. Micropatterning traction forces in living cells. Cell Motil Cytoskeleton 2002; 52: 97–106.
34. Wang N, Tolic-Norrelykke IM, Chen J et al. Cell prestress. I. Stiffness and pretress are closely associated in adherent contractile cells. Am J Physiol Cell Physiol 2003; 282: C606–16.
35. Wang N, Butler JP, Ingber DE. Mechanotransduction across the cell surface and through the cytoskeleton. Science 1993; 260: 1124–7.
36. Maniotis A, Chen C, Ingber DE. Demonstration of mechanical connections between integrins, cytoskeletal filaments and nucleoplasm that stabilize nuclear structure. Proc Natl Acad Sci USA 1997; 94: 849–54.
37. Choquet D, Felsenfeld DP, Sheetz MP. Extracellular matrix rigidity causes strengthening of integrin-cytoskeleton linkages. Cell 1997; 88: 39–48.
38. Chrzanowska-Wodnicka M, Burridge K. Focal adhesions, contractility and signaling. Annu Rev Cell Dev Biol 1996; 12: 463–518.
39. Balaban NQ, Shwarz US, Riveline D et al. Force and focal adhesion assembly: A close relationship studied using elastic micropatterned substrates. Nat Cell Biol 2001; 3: 466–72.
40. Riveline D, Zamir E, Balaban NQ et al. Focal contacts as mechanosensors: Externally applied local mechanical force induces growth of focal contacts by an mDia1-dependent and ROCK-independent mechanism. J Cell Biol 2001; 153: 1175–86.
41. Folkman J, Moscona A. Role of cell shape in growth control. Nature 1978; 273: 345–9.
42. Adam LP, Hathaway DR. Identification of mitogen-activated protein kinase phosphorylation sequences in mammalian h-caldesmon. FEBS Lett 1993; 322: 56–60.
43. Huang S, Ingber DE. The structual control mechanical complexity of cell-growth control. Nat Cell Biol 1999; 1: E131–8.
44. Korff T, Augustin HG. Tensional forces in fibrillar extracellular matrices control directional capillary sprouting. J Cell Sci 1999; 112: 3249–58.
45. Grove AD, Prabhu VV, Young BL et al. Both protein activation and gene expression are involved in early vascular tube formation *in vitro*. Clin Cancer Res 2002; 8: 3019–26.
46. Roskelley CD, Srebrow A, Bissell MJ. A hierarchy of ECM-mediated signalling regulates tissue-specific gene expression. Curr Opin Cell Biol 1995; 7: 736–47.
47. Boudreau N, Werb Z, Bissell MJ. Suppression of apoptosis by basement membrane requires three-dimensional tissue organization and withdrawal from the cell cycle. Proc Natl Acad Sci USA 1996; 93: 3509–13.
48. Weaver VM, Lelievre S, Lakins JN et al. Beta4 integrin-dependent formation of polarized three-dimensional architecture confers resistance to apoptosis in normal and malignant mammary epithelium. Cancer Cell 2002; 2: 205–16.
49. Moore KA, Huang S, Kong Y et al. Control of embryonic lung branching morphogenesis by the Rho activator, cytotoxic necrotizing factor 1. J Surg Res 2002; 104: 95–100.
50. Harding TC, Geddes BJ, Murphy D et al. Switching transgene expression in the brain using an adenoviral tetracycline-regulatable system. Nat Biotech 1998; 18: 553–5.